Eurasian Journal of Analytical Chemistry
ISSN: 1306-3057 OPEN ACCESS 2019 14 (3): 35-47

Experimental and Kinetic Studies on Adsorption of Trace Amount of Nickel from Aqueous Solutions Using a New Chelating Adsorbent Polystyrene (4-azo-1')-2'-hydroxy-5'-sulfobenzene

Ali Saad Alwesabi, Badr Ismael Alabsi*

Received: 19 June 2019 ▪ Revised: 17 July 2019 ▪ Accepted: 14 August 2019

Abstract: The modern instrumental analysis methods do not always allow direct determination of trace amounts of elements due to influence of the matrix composition of the sample. A novel polystyrene (4-azo-1')-2'-hydroxy-5'-sulfobenzene abbreviated as PSAHSB adsorbent synthesized based on amino polystyrene functionalized with chelating azo phenolic groups was applied for removal of trace Ni (II) ions from aqueous solutions under batch conditions. The parameters including pH, temperature and contact time on removal of nickel ions were studied extensively. The ionization constants of an adsorbent were investigated. The adsorption isotherm, thermodynamics and kinetics parameters were also investigated. To gain insight into the adsorption kinetics, both the pseudo-kinetics were examined. The adsorption of trace nickel ions increased smoothly in the pH range of 1–3, then remained at a higher level for the pH range of 3–7.5, but decreased sharply at pH large than 8, which demonstrated that the adsorption was affected strongly by pH. On the other hand, the adsorption capacity was increased sharply with the temperature rising. The adsorption equilibrium time could be reached in 25min. The equilibrium data could fit the Langmuir isothermal model very well, and the thermodynamic analysis suggested that the adsorption of nickel ions on the adsorbent is a spontaneous and endothermic process. The results indicated the pseudo-second-order kinetic model fitted the experimental data better. The adsorbent have three ionization constants and exhibits excellent stability and high regeneration. The absorbent can be used efficiently for treatment of Ni^{+2}ions from naturally- occurring and industrial materials.

Keywords: Polystyrene Azo Phenoliccomplex, Preconcentration, Adsorption and Desorption, Kinetics and Thermodynamics, Dissociation Constants.

INTRODUCTION

The detection of toxic metal ions in aquatic ecosystems is an important global issue because these contaminants may have harmful effects on plants, animals, humans and ecosystem [1].Among the most toxic metallic water pollutants in aquatic environments is nickel[2].Nickel (Ni) is the most common metals causing skin contact allergy, affecting about 10–20% of the general population[3]. According to the WHO guidelines, the maximum permissible concentration of nickel in industrial wastewaters is 4.1 mg/L,

Ali Saad Alwesabi, Pharmaceutical Science Department, Faculty of Pharmacy, University of Science and Technology, Sana'a, Yemen. E-mail: alialwesabi99@gmail.com
Badr Ismael Alabsi*, Chemistry Department, Faculty of Science, Hodeida University, Hodeida, Yemen.
E-mail: badrasml@gmail.com

while that in drinking water should be less than 0.1 mg/l [4].Therefore, it is essential to reduce or remove Ni(II) from industrial wastewaters before discharging them into the environment.

The detection of heavy metals in low concentrations is a difficult task; however, it can be achieved with existing advanced analytical methods, such as high-performance liquid chromatography (HPLC), inductively coupled plasma mass spectroscopy (ICP-MS), atomic emission or atomic absorption spectroscopies (AES, AAS), cold vapor atomic fluorescence spectroscopy (CVAFS), electro-deposition, chemical precipitation and ion exchange process [5-8]. These methods are extremely sensitive but very expensive, most of them require multi-step processing, sometimes ineffective particularly when the metal concentration is less than 100 µg/ml, and require specialized laboratory conditions and highly trained personnel [9][9]. As a result, both the time and cost of the analysis are very high. An alternative approach uses chelating polymer adsorbents, which can be respected as the most common methods for the removal of hazard heavy metals from the aqueous solutions by cause of their lower costs, high removal efficiency, robustness and biodegradability, especially for metal ions at levels $10^{-5}-10^{-8}$%[7, 9, 10].Using of chelating polymer adsorbents for removal of metal ions from aqueous solution has been widely studied[[11-18].The important characteristic of these adsorbents depends on the active chelating positions, which have ability of chelating about metallic ions during complication processes[14-16, 18].

A new class of chelating polymer adsorbents have been synthesized based on amino-polystyrene functionalized with chelating azo-2'-hdroxy groups which are insoluble in water, acids, alkalis, and organic solvents and undergo regeneration 9-11 working chemisorption cycles [17].

The main goal of this work is to investigate the removal of Ni(II) ions from simulated aqueous solutions by using new chelating adsorbent Polystyrene (4-azo-1')-2'-hydroxy-5'-sulfobenzene PSAHSB powder, which belongs to derivatives of polystyrene azo phenoliccomplexes. The parameters affecting on the adsorption efficiency such as pH, initial nickel ion concentration, contact time and temperature were extensively investigated. Moreover, the ionization constants of acidic groups of adsorbent were invigilated. The Langmuir and Freundlichmodels were employed for analysis of the adsorption equilibrium. The adsorption kinetics of Ni (II) on PSAHSB also were evaluated.

EXPERIMENT

Preparation of Adsorbent

We applied PSAHSB adsorbent to adsorb trace amount of nickel ions from the simulated aqueous solutions. The structure of this adsorbent presented in Fig.1. The adsorbent was purchased from of IGEM Laboratories, Russia. The adsorbent was synthesized according to procedures in [19-21].The synthesis included four successive stages *i*)nitration of a polystyrene to polynitrostyrene; ii) reduction of this product to polyaminopolystyrene; *iii*) diazotization of the produced amino group; *iiii*) azo-coupling of the diazotized amino with monomeric 4-hydroxybenzenesulfonic acid ligand. The adsorbent is insoluble in water, acids, alkalis, and organic solvents and do not swell. The absorbent was ground in an agate mortar and bolted through a sieve of convert 200 meshes (74µm) [[22].

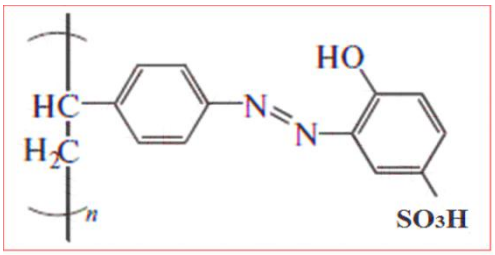

Fig.1: Chemical structure of the PSAHB-SO3H adsorbents

Structure Characterization

The PSAHSB adsorbent is characterized by *i)* Atomic force microscopy (AFM) (Multimode NS3a,No. 3327, America) ; *ii)* Fourier transform infrared (FTIR) (Perkin Elmer SpectrumBX FT-IR, Japan) in pressed KBr pellets (spectral resolution: 1 cm−1);iii) potentiometric determination of content of chelating groups and the dissociation constants of the adsorbent.

Adsorption Experiments

The adsorption of Ni (II) ions on PSAHSB adsorbent was performed by batch methods under ambient conditions. 25mg of adsorbent was added into 25 mL of Ni (II) solutions in different initial concentrations with stirred at 300 rpm. An adsorbate onto adsorbent were separated from mixture by filtration using

0.45 µm filter paper. The effect of pH and time on Ni (II) adsorption was screened in detail. The pH was adjusted up to the desired value with either 0.1M HCl or 0.1MNaOH solutions by using pH meter (781 pH/Ion meter). The adsorption isotherms, which indicate the Ni (II) ions adsorption behavior, were investigated at 293.15, 313.15 and 333.15 K, respectively. The residual concentration of nickel ions in the filtrate $C_e$was determined by using a UV–vis spectrophotometer (LI-295 UV-VIS) with H_2Dm reagent [[23] at λ=445 and by using the earlier constructed calibration curves. The equilibrium adsorption capacity qe (mg.g-1) and degree of adsorption (R,%) were calculated according to the Eq.1,2[24].

$$q_e = \frac{(C_0 - C_e)\ V}{w} \qquad \text{Eq.1}$$

$$R,\% = \frac{C_0 - C_e}{C_0} \times 100 \qquad \text{Eq.2}$$

Where C_0 and C_e are initial and equilibrium concentrations of Ni(II) in the solution (mg.L^{-1}) respectively. *V*is the solution volume (L), *w* is the adsorbent mass (g).Experiments were carried out in triplicate, and average value was taken.

Adsorption Kinetics

In order to investigate the kinetic mechanism of theadsorption process, two kinds of kinetic models were applied to describe the experimental data ofthe adsorption kinetics. The pseudo-first-order kinetics model is one of the most broadly used to describe the adsorption of metal ions from aqueous solutions [25-27]. The linear form of pseudo-first-order equation was expressed by Eq.3.

$$\log(q_e - q_t) = \log q_e - (\frac{K_1}{2.303})\ t \qquad \text{Eq.3}$$

Where q_e and q_t (mg/g) are the adsorption capacity at equilibrium and time *t* respectively, and k_1(tim.$^{-1}$) is the rate constant of the pseudo-first-order model.

The other one is the pseudo-second order model. The linearity of this model given by Eq.4 [28].

$$\frac{t}{q_t} = \frac{1}{(K_2 . q_e^2)} + \frac{t}{q_e} \qquad \text{Eq.4}$$

whereK_2 ($g.mg^{-1}\min^{-1}$) is rate constant of the pseudo-second order model.

Desorption and Recycle Test

Study of desorption for regeneration of the adsorbent is necessary to make the adsorption process more economical. Therefore**,** desorption of adsorbate from the adsorbent was carried out by washing it to a beaker with 10 mL of *1 to 4 M* concentrations of HCl and HNO_3 desorbing agents. Then, the system mixed using a magnetic stirrer for 1hour. Degree of desorption (D,%) of ions from the adsorbent was determined by Eq.5.

$$D,\% = \frac{C_i - C_d}{C_i} \times 100 \qquad \text{Eq.5}$$

Where C_i is concentration of adsorbed Ni(II)was predetermined and C_d is concentration of adsorbed Ni(II) in acidic solution.

RESULTS AND DISCUSSIONS

Characterization of adsorbent

1) FTIR Analysis before and After Ni Complexation

The FTIR spectrum of PSAHSB adsorbent was shown in Fig. 2(a).The FTIR spectrum of this adsorbent confirmed the presence of functional groups characteristic of adsorbent. Hydroxyl group was identified by the broad band attributed to stretching vibrations of O–H bonds in the range 3600–3100 cm^{-1}, the signals at 2925, 1600, 1450,1110, 854, 700, cm^{-1} associated with 2-phthol-4-sulfonic acid moiety (phenyl). The peak at 1519 cm^{-1} is because of the stretching vibrations of (–N=N–) onds and the peak at

3060 cm^{-1} attributed to Ar–H, signal at 1350 cm^{-1} associated with the stretching vibrations of C–OH groups in the structure of adsorbent[29]. The presence of aliphatic structure is attributed to the stretching vibrations of C-H bonds in the range 2940–2850 cm^{-1}. The signal 710– 680 cm^{-1} associated with deformation vibrations of C–C groups in the benzene ring. Thus, the IR spectrum confirms the structure of the adsorbent in Fig. 1.

The IR spectrum of the PSAHSB adsorbent and its complex with Ni (II) is shown in Fig. 2(b). In this study a processes is proposed based on ion exchange by the following active chlating groups: negativelly charged of phenolic oxygen atom with positively charged of Ni(II) ions.The groups are capable of bonding Ni(II) ions during the dissociation of a H^+ cations[12, 30]. Based on the FT-IR spectra obtained, it can be deduced that after the adsorption, the intensity of the relevant bands is reduced (hypsochromic shift). This is visible in the stretching vibrations of -OH groups in the range 3560–3350 cm^{-1} and the vibrations of –N=N- groups shifeted to the 1508 cm^{-1}. The obtained signles in IR spectra show visibly that Ni(II) ions form bonds with oxygen groups, at the same time causing separation of a H^+ cation. Verification of this are slightly shifts in the wave numbers of the signals following the interactions of Ni(II) ions with active chelating groups on adsorbent surface. For example, maximal wave number for the signal -OH groups, is around 3420 cm^{-1}, and after adsorption of nickel ions is shifted to the 3385 cm^{-1}. Similar, the maximal wave number for signal N=N groups is around 1519 cm^{-1} before adsotption and after wes shifted to the 1508 cm^{-1}[12, 30].

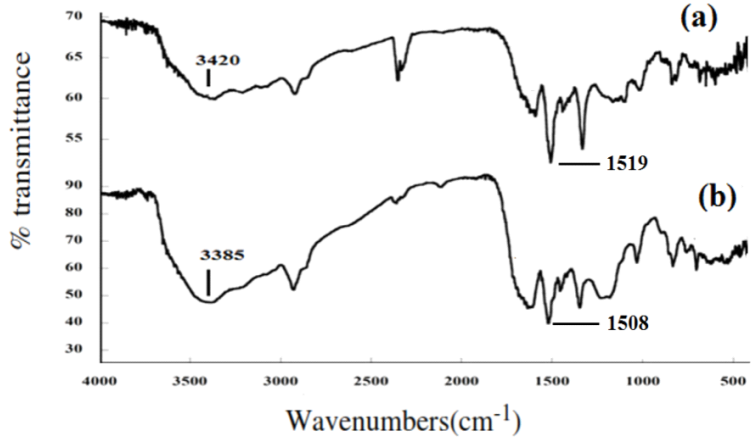

Fig.2: FT-IR spectra before (a) and after (b) the adsorption of nickel (II) onto PSAHSB adsorbent

2) Surface Morphology

Fig. 3(a) shows scanning force microscopy SFM image of the initial surface of the adsorbent under study[31]. There is occasional horizontal interference that indicates the presence of a small number of particles with low adhesion on the surface that are displaced by the probe at scanning. We can clearly see the globular structure of the surface of adsorbent Fig.1 (b). The adsorbent was grains with *a* grain size in the range of 50 - 160 nm, and a pore size in the range of 10 to100 nm. This essentially led to the formation of mixed meso/ macro-pores[32].

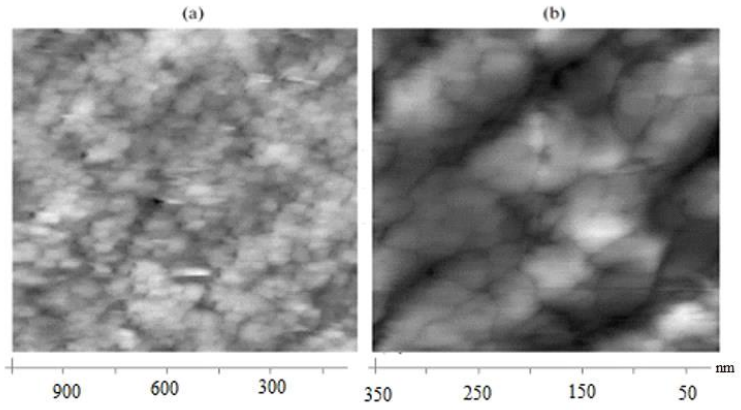

Fig. 3: SFM image of a adsorbent surface in 2D (a) 725 × 725pixels (b) 1200 × 1200 pixels

3) Acidic Properties of the Adsorbent

The determination of acidic dissociation constants is an essential step in the examination of the physic-chemical properties of chelating polymer adsorbents. The of adsorbents play a fundamental role in many analytical procedures such as acid-base titration, solvent extraction, stability, complex formation, determine the pH range in which these groups are ionized and capable of participating in reactions of ion exchange[33].

The direct potentiometric titration of adsorbent was carried out according *to*[34-36]. From Fig. 4, it can be noticed that the differential titration curve of ΔpH/ΔQ – Q for adsorbent exhibit three jumping *positions* (inflection points), which can be attributed to the ionization of the betainic protons of the N=N- (1), -SO_3H (2) and –OH (3) groups during the titration of adsorbent. These results unambiguously confirmed the chemical structure of adsorbent in (Fig.1).

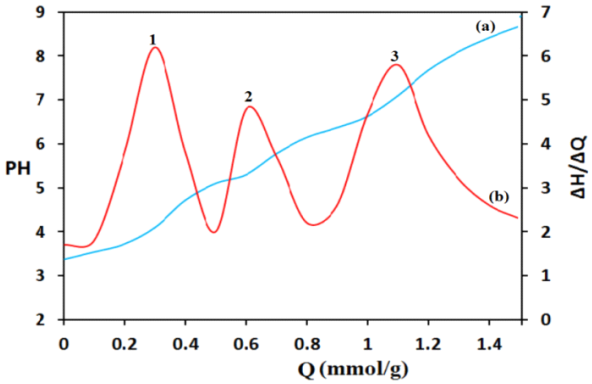

Fig. 4: (a) Integral and (b) differential curves of potentiometric titration for adsorbent [μ = 1 M KCl; 0.02 M of NaOH; t=24 h; T=298K; Q is degree of neutralization of functional groups]

Dissociation constants of the chelating groups were determined by data of potentiometric titration and using the Henderson-Hasselbach equation in (Eq.6)[37].

$$pK_{ion} = pH - n.\log(\frac{\alpha}{1-\alpha}) \qquad \text{Eq.6}$$

The pK_{ion} values of ionized groups were shown in Fig.5, and reported in table 1. It clear that the pK_{ion} values were relatively medium, which enhanced the affinity between the element ions and the adsorbents, that made the adsorption faster and form more stable complexes.

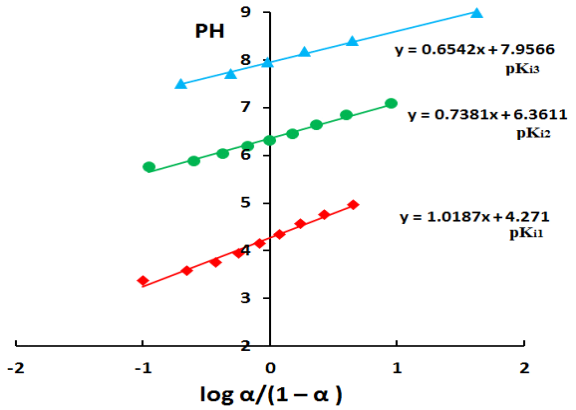

Fig.5: Determination of dissociation constants for PSAHSBby the graphical method

Table 1: Ionization constants (pK_{ion})of chelating groups of PSAHSB adsorbent

Ionization stages (IS)	pK_{ion} (graphical)	pK_{ion}(calculated), *n*=3¶		
			S_r	±δ
pK_{i1} of 1st IS of –N=N-	4.27	4.11	0.01	4.13±0.05
pK_{i2} of 2nd IS of –SO3H	6.36	6.31	0.007	6.13±0.03
pK_{i3} of 3th IS –OH	7.96	8.03	0.006	8.03±0.04

¶the mathematical results were expressed as ±st/$n^{1/2}$ where is the mean of *n* observations, *s* is the standard deviation, *t* is distribution value chosen for 95% confidence level and S_r is the relative standard deviation.

Effect of pH and Initial Ni (II) Concentration

The pH of the nickel solution plays a majorrole in all adsorption process, especially on the adsorption capacity. The degree of adsorption is significantly affected by surface charge of the adsorbent, which is highly dependent on the pH of the solution [38]. The optimal pH for the ideal adsorption was determined experimentally from the plot of adsorption degree (R %) versus pH in range from 1 to 10. Fig. 6 shows the effects of pH on the adsorption of Ni (II) ions onto PSAHSB adsorbent. The degree of adsorption (R, %) was calculated to be 96.2% in the pH range of 3 to 7. At low pH, the R% was low also, due to the increase in the positive charges on the surface of polymer (i.e. active chelating sites of $N=NH^{+}$, $C\text{-}OH_2^{+}$ in acidic form), leading up to electrostatic repulsion between the Ni^{2+} ions and these active sites on the adsorbent surface. The increase in pH leads to decrease in electrostatic repulsion because of reduction in the positively charged surface, thus resulting in higher adsorption[39]. In the basic solution at pH large than 7, the adsorbent surface becomes negatively charges, and the degree of adsorption decreased rapidly where Ni^{2+} ions precipitated as nickel hydroxide.

As shown in Fig. 6, it is clear that the adsorption of Ni ions increased with increase in initial Niconcentration. Increasing concentration gradient, acts as increasing the driving force, and in turn leads to an increase in equilibrium adsorption until adsorbent saturation is reached.

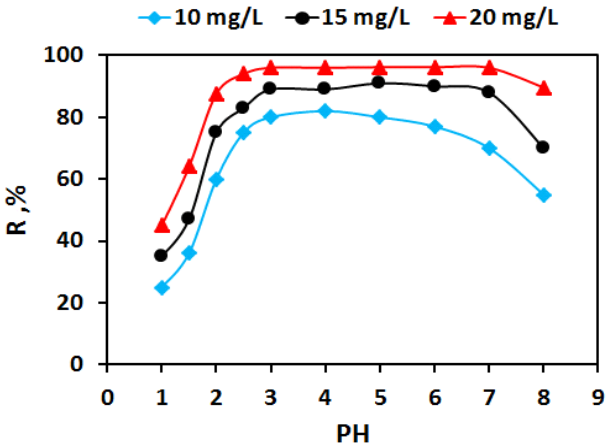

Fig. 6: Effect of pH on the adsorption of Ni(II) on 20 mg PSAHSB adsorbent, 300 rpm, 90 min &298.5 K.

Effect of Contact Time

The adsorption of Ni (II) on the adsorbent was achieved in less than 20 min at 298.15K as shown in Fig.7. The removal amounts of Ni ions by PSAHSB adsorbent was maintained in the same rate even extending the contact time. Noteworthy, the degree of adsorption was calculated to be 96.2 % at concentration 0.96 μg /mL of nickel ions. Based on these results, PSAHSB adsorbent was proved to be an efficient adsorbent possessing relatively large adsorption capacity. An increase in the temperature to 60°C shortened the time of adsorption but led to the partial degradation of formed complex and a decrease in the value of Ras the result shown in Fig. 7.

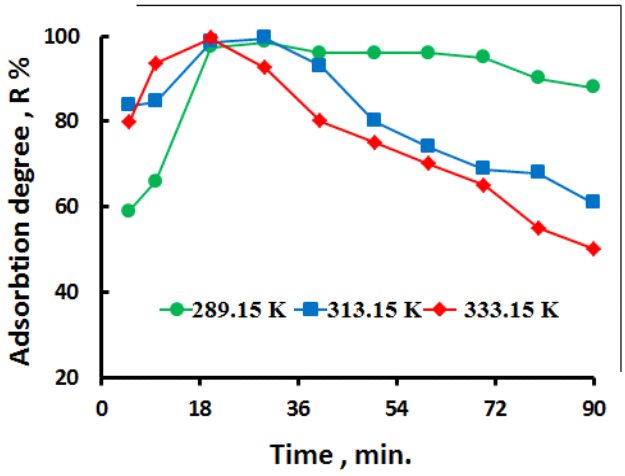

Fig. 7: Effect of contact time on the adsorption equilibrium at different temperatures, PH =5.5

Adsorption Kinetic

The liner plot of $\log(q_e - q_t)$ vs.t for the pseudo-first-order model, and $\frac{t}{q_m}$ vs. t for the pseudo second-order model were shown in Fig.8 (a,b).The parameters of the two models were shown in Table. 2. The results suggested that the experimental data were fitted to the pseudo second-order kinetic model. By comparison of experimental and calculated q_e values, the q_e of this model is more approximate to the experimental data and the correlation coefficients is 0.999 which is very close to 1. In Table. 2, the rate constant of the pseudo second-order model (k_2) is very small (0.02/min) indicating that the adsorption equilibrium can occur in a short time.

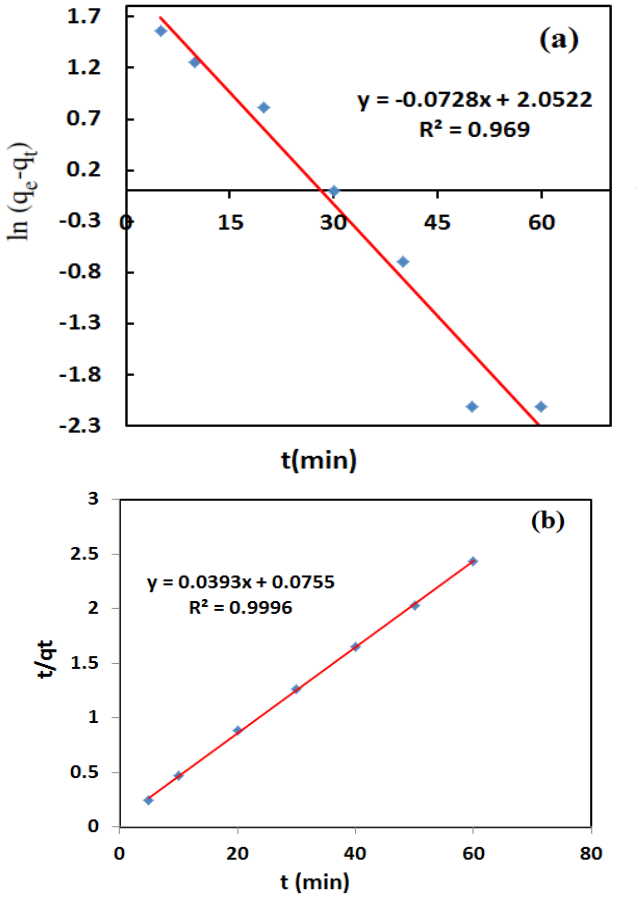

Fig. 8: Kinetic model for Ni (II) adsorption.(a) Pseudo-first-order, (b) pseudo-second order models [initial Ni(II) conc. = 25 mg/L; contact time = 5–90 min; T=298K; V=25ml; pH=6]

Table 2: The obtained parameters of pseudo-first – order and pseudo-second–order models

Kinetic models		Pseudo-first-order kinetic model			Pseudo-second-order kinetic model		
Parameters	q_e (exp.)	q_e (cal.) mg/g)	k_1 (1/min)	R^2	q_e(cal.) (mg/g)	k_2 (1/min)	R^2
Values	24.05	7.8	-0.073	0.875	25.4	0.02	0.999

Adsorption Isotherm

The fitting of adsorption data to a isotherm is important to both theoretical and practical applications. In order to optimize the adsorption system, it is essential to establish the most appropriate correlations of the equilibrium data of each system [40] Equilibrium isotherm equations are used to describe the experimental adsorption data. The adsorption isotherms are important data to understand the adsorption mechanism[41]. In this work, three different temperatures at initial pH = 6 ± 0.02 for each isotherm were used to describe the adsorption isotherms presented in Fig.9.

The Langmuir and Freundlich models were applied to correlate the experimental data [42, 43].The Langmuir model is based on the assumption that the maximum adsorption occurs when saturated monolayer of solute molecules is present on the adsorbent surface, the energy of adsorption is constant and here is no migration of adsorbate molecules in the surface plane. The equation of Langmuir adsorption model was expressed in linear form by (Eq.7).

$$\frac{C_e}{q_e} = \frac{1}{q_m . K_L} + \frac{C_e}{q_m} \qquad \text{Eq.7}$$

Where q_m (mg/g), and K_L are the Langmuir constants related to affinity towards to the adsorbent and to heat of adsorption (L/mg), respectively.

The results indicated that higher temperature did favor to the adsorption of Ni (II) ions on PSAHSB where as this behavior was diminished at lower temperature.

The Freundlich model assumes that different sites with several adsorption energies are involved. The equation of Freundlich adsorption model was expressed in linear form as Eq.8[41].

$$\log q_e = \log K_F + \frac{1}{n_F} \log C_e \qquad \text{Eq.8}$$

where $1/n_F$ and K_F are the Freundlich constants, K_F and n_F are the indicators of the adsorption capacity and heterogeneity of the process, respectively. According to the Freundlich model assumptions, if n_F less than 1, the adsorption process is unfavorable, while if 1 <n_F> 10, the adsorption process is favorable [44]. The experimental data of Ni (II) ions adsorption (Fig. 9) were regressively analyzed with the Langmuir and Freundlich adsorption model (Fig. 10 a & b) with the relative values calculated from the two models in Table 3. It can be concluded that Langmuir adsorption model coincides with the experimental data better than Freundlich adsorption model, which indicates that the Langmuir isotherm with complete monolayer coverage of the adsorbent particles can fit the experimental data very well[45].

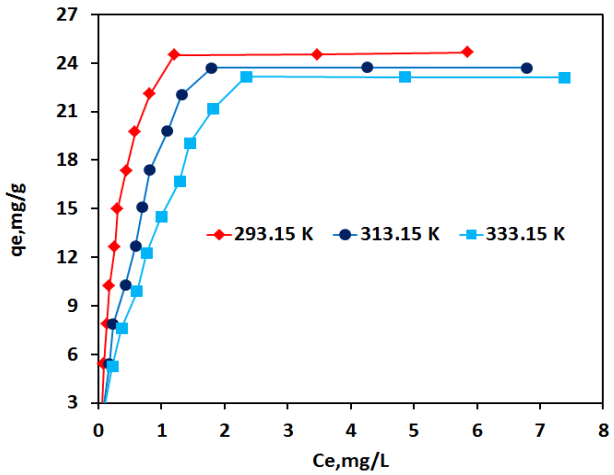

Fig. 9: Adsorption isotherms of Ni(II) ions on PSAHSB adsorbent at three different temperatures, [initial Ni(II) conc. = 0.01 – 1.5 mg/L; pH = 0; Adsorbent dose = 25 mg ;t = 20 min]

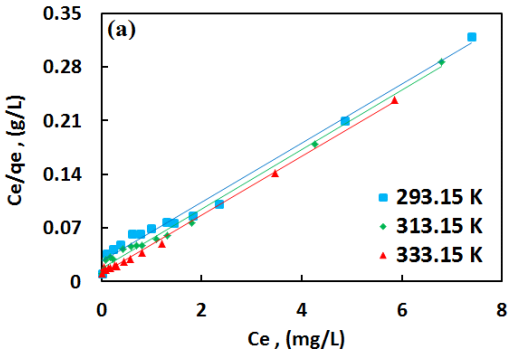

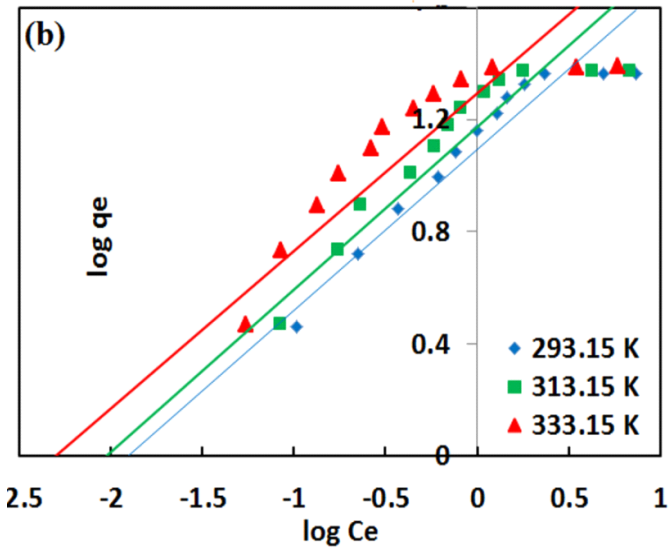

Fig. 10: Langmuir (a) and Freundlich (b) isotherms for Ni(II) ions adsorption on PSAHSBat different temperatures.

Table 3: Summary of the isotherm constants and the correlation coefficients for different isotherms

T(k)	Langmuir isotherm			Freundlich isotherm		
	q_m (mg/g)	K_L (L/mg)	R^2	K_F(mg/g)	n_F (g /L)	R^2
293.15	25.9	0.056	0.986	12.39	1.74	0.959
313.15	25.9	0.084	0.992	14.91	1.73	0.931
333.15	26.0	0.154	0.997	19.90	1.77	0.862

3.6. Adsorption Thermodynamics

The thermodynamic parameters such as free energy (ΔG^0), enthalpy (ΔH^0) and entropy (ΔS^0) for nickel ions adsorption on our adsorbent can be calculated from the temperature dependent adsorption. The values of ΔH^0 and ΔS^0 can be calculated from Eq.9&10.

$$K_d = \frac{(C_0 - C_e)}{C_e} . \frac{V}{m} \qquad \text{Eq. 9}$$

$$\ln K_d = \frac{\Delta S^0}{R} - \frac{\Delta H^0}{RT} \qquad \text{Eq. 10}$$

where R (8.3145 J.mlo^{-1}.K^{-1}) is the ideal gas constant. ΔH^0 and ΔS^0 were calculated from the slope and intercept of Von't Hoff plots of *ln* K_d vs. 1/T (Fig.11).

The Gibbs free energy (ΔG^0, J) of specific adsorption was obtained from Eq.11[46].

$$\Delta G^0 = \Delta H^0 - T\,\Delta S^0 \qquad \text{Eq.11}$$

The thermodynamic parameters (ΔG^0, ΔH^0 and ΔS^0) calculated from temperature dependence were presented in Table 4.The positive value of ΔH^0 confirms the endothermic nature of the adsorption process[47].

The endothermic nature was also demonstrated by the adsorption isotherms at three different temperatures. One possible interpretation for this adsorption enthalpy was that Ni (II) ions were solvated in water. When these ions get adsorbed, they are to some extent denuded of their hydration sheath. This dehydration process of ions requires energy[42]. The ΔG^0 was negative as expected for a spontaneous process under the conditions applied. The decreases in free energy with the increase of *T* indicated more efficient adsorption at high temperature. The positive value of ΔS^0 reflects the affinity of PSAHSB toward Ni (II) ions in aqueous solutions and may suggest some structural changes in adsorbate and adsorbent.

Similar results have been previously published [41, 48, 49]. The result of Ni (II) ions adsorption on PSAHSB was a spontaneous and endothermic process.

Table 4: Thermodynamic parameters for the adsorption of Ni^{+2} onto PSAHSB with different Ni(II) initial concentrations, *t* =20 min

C_0(mg/L)	ΔH^0(KJ/ml)	ΔS^0(J/mol.K)	ΔG^0(KJ/mol)		
			293.15K	313.15K	333.15K
10	23.31	110	-32.20	-34.40	-36.6
15	22.19	108	-31.60	-33.70	-35.9
20	21.04	103	-30.03	-32.08	-34.1

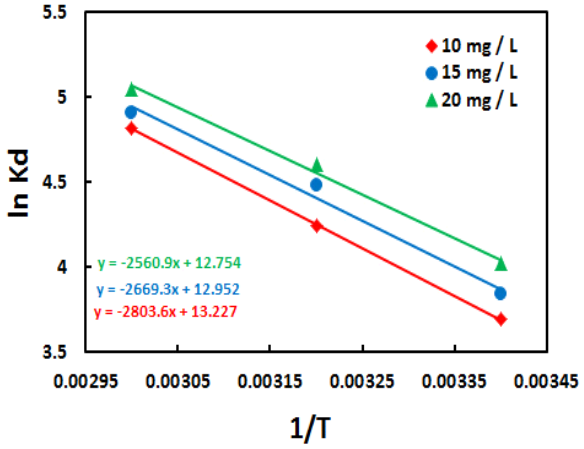

Fig. 11: Effect of temperature on the distribution coefficients of Ni onto PSAHSB adsorbent at different initial Ni solution concentrations.

Desorption and Regeneration Studies

As shown in Fig.12 (b), thatHNO3 is a weak desorbing agent. This is evidence of a strong bond between the adsorbate and adsorbent. Only when hydrochloric acid was used; a significant increase in the degree of desorption was realized. It was found that as the concentration of the hydrochloric acid increased, there was an improvement in the effectiveness of the adsorbent regeneration process. The mechanism of desorption is based on the exchange of hydrogen ions H^+ with the adsorbed Ni (II) ions.

The cyclic adsorption–desorption tests are also carried out to evaluate the regeneration ability with results shown in Fig. 12(a). The degree of adsorption was basically maintained at a level higher than 90% for each cycle after desorption with 12 cycles, which proved the high regeneration ability of thePSAHSB adsorbent.

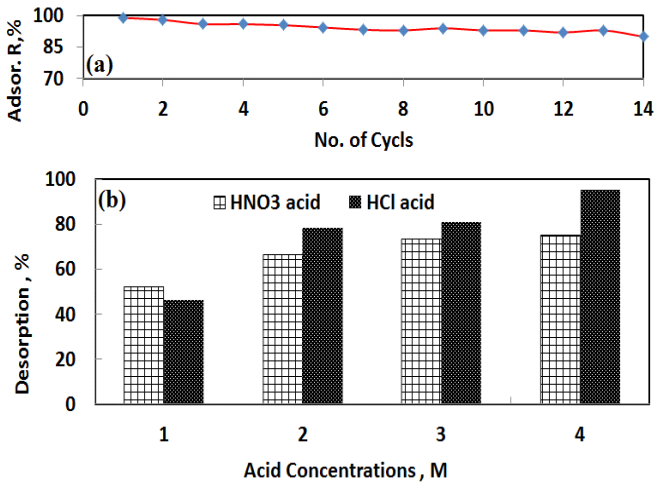

Fig. 12: (a)Adsorption of Ni on PSAHSB in 12 cycles of adsorption–desorption.(b)Desorption studies of adsorbent at 298K (metal ion concentration=25 mg/L, adsorbent dose=205mg, and pH=6).

CONCLUSION

A +new low-cost polystyrene (4-azo-1')-2'-hydroxy-5'-sulfobenzene adsorbent was applied to investigate the removal of Ni $^{2+}$from aqueous solutions. Optimum pH of adsorption was *located* in the *range* of 3- 7.The adsorption capacities of Ni ions on adsorbent are enhanced with the increasing of the pH value, nickel content and temperature of the solution. The adsorption equilibrium could be reached within 20 min. Moreover, the Langmuir isotherm model fitted the experimental data very well, and the high stability and remarkable regeneration ability indicated that the PSAHSB adsorbent is a promising adsorbent for the removal of Ni^{2+} from aqueous solutions.

ACKNOWLEDGMENTS

This work was financially supported by University of Science and Technology (UST), Sana'a, Yemen according to decision No.2014/15/N/ ST8/00319.

REFERENCES

[1] Abu-Ali, H., Nabok, A., & Smith, T. J. (2019). Development of novel and highly specific ssDNA-Aptamer-based electrochemical biosensor for rapid detection of Mercury (II) and Lead (II) ions in water. *Chemosensors*, *7*(2).

[2] Abu-Ali, H., Nabok, A., Smith, T., & Al-Shanawa, M. (2017). Inhibition biosensor based on DC and AC electrical measurements of bacteria samples. *Procedia technology*, *27*, 129-130..

[3] Chen, J. K., & Thyssen, J. P. (Eds.). (2018). Metal Allergy: From Dermatitis to Implant and Device Failure. *Springer*.

[4] Gupta, S., & Kumar, A. (2019). Removal of nickel (II) from aqueous solution by biosorption on A. barbadensis Miller waste leaves powder. *Applied Water Science*, *9*(4).

[5] Saidur, M. R., Aziz, A. A., & Basirun, W. J. (2017). Recent advances in DNA-based electrochemical biosensors for heavy metal ion detection: a review. *Biosensors and Bioelectronics*, *90*, 125-139.

[6] Meena, A. K., Kadirvelu, K., Mishra, G. K., Rajagopal, C., & Nagar, P. N. (2008). Adsorptive removal of heavy metals from aqueous solution by treated sawdust (Acacia arabica). *Journal of hazardous materials*, *150*(3), 604-611.

[7] Ramezankhani, R., Sharif, A. A. M., Sadatipour, M. T., & Abdolahzadeh, R. (2008). A mathematical model to predict nickel concentration in karaj river sediments. *Journal of Environmental Health Science & Engineering*, *5*(2), 91-94.

[8] Khellaf, N., & Zerdaoui, M. (2009). Growth response of the duckweed Lemna minor to heavy metal pollution. *Journal of Environmental Health Science & Engineering*, *6*(3), 161-166.

[9] Ghasemi, N., Ghasemi, M., Mashhadi, S., & Trraf, M. H. (2012). Kinetics and isotherms studies for the removal of Ni (II) from aqueous solutions using Rosa canina L. In *International Congress on Informatics, Environment, Energy and Applications-IEEA*, *38*.

[10] Zaira, Z. C., Sharifuddin, M., Rashid, A. K., & Abdulbari, A. A. (2011). Equilibrium kinetics and isotherm studies of Cu (II) adsorption from waste water onto alkali activated Oil Palm Ash. *American Journal of Applied Sciences*, *8*(3), 230-237.

[11] Kumar, R., Kumar, M., Ahmad, R., & Barakat, M. A. (2013). l-Methionine modified Dowex-50 ion-exchanger of reduced size for the separation and removal of Cu (II) and Ni (II) from aqueous solution. *Chemical engineering journal*, *218*, 32-38.

[12] Wu, N., & Li, Z. (2013). Synthesis and characterization of poly (HEA/MALA) hydrogel and its application in removal of heavy metal ions from water. *Chemical Engineering Journal*, *215*, 894-902.

[13] Lin, Z., Zhang, Y., Chen, Y., & Qian, H. (2012). Extraction and recycling utilization of metal ions (Cu2+, Co2+ and Ni2+) with magnetic polymer beads. *Chemical engineering journal*, *200*, 104-112.

[14] Zhu, Y., Hu, J., & Wang, J. (2012). Competitive adsorption of Pb (II), Cu (II) and Zn (II) onto xanthate-modified magnetic chitosan. *Journal of hazardous materials*, *221*, 155-161.

[15] Abd El-Moniem, N. M., El-Sourougy, M. R., & Shaaban, D. A. F. (2005). Heavy metal ions removal by chelating resin. *Pigment & resin technology*, *34*(6), 332-339.

[16] Monier, M., Ayad, D. M., & Abdel-Latif, D. A. (2012). Adsorption of Cu (II), Cd (II) and Ni (II) ions by cross-linked magnetic chitosan-2-aminopyridine glyoxal Schiff's base. *Colloids and Surfaces B: Biointerfaces*, *94*, 250-258.

[17] Basargin, N. N., Kosolapova, N. I., Anikin, V. Y., & Rozovskii, Y. G. (2007). Sorption of phosphorus (V) by polymeric sorbents based on aminopolystyrene and 4-amino-N-azobenzenesulfamide. *Russian Journal of Inorganic Chemistry*, *52*(10), 1638-1642.

[18] Atia, A. A., Donia, A. M., & Shahin, A. E. (2005). Studies on the uptake behavior of a magnetic Co3O4-containing resin for Ni (II), Cu (II) and Hg (II) from their aqueous solutions. *Separation and purification technology*, *46*(3), 208-213.

[19] Basargin, N. N., Zueva, M. V., Rozovskii, Y. G., & Pashchenko, K. P. (2005). Preconcentration of gold on chelating polymer adsorbents and its determination in rocks and ores. *Journal of Analytical Chemistry*, *60*(3), 234-239.

[20] Shyaa, A. A. (2012). Synthesis, Characterization and Thermal Study of Polyimides Derived from Polystyrene. *Journal of university of Anbar for Pure science*, *6*(1), 21-27.

[21] Philippides, A., Budd, P. M., Price, C., & Cuncliffe, A. V. (1993). The nitration of polystyrene. *Polymer*, *34*(16), 3509-3513..

[22] Shaaban, A. F., Fadel, D. A., Mahmoud, A. A., Elkomy, M. A., & Elbahy, S. M. (2014). Synthesis of a new chelating resin bearing amidoxime group for adsorption of Cu (II), Ni (II) and Pb (II) by batch and fixed-bed column methods. *Journal of Environmental Chemical Engineering*, *2*(1), 632-641.

[23] Shpigun, L. K., Kolotyrkina, I. Y., & Zolotov, Y. A. (1986). Flow-Injection Analysis-Spectrophotometric Determination of Nickel. *Journal of Analytical Chemistry of the Ussr*, *41*(7), 925-928.

[24] Ajmal, M., Rao, R. A. K., Ahmad, R., & Ahmad, J. (2000). Adsorption studies on Citrus reticulata (fruit peel of orange): removal and recovery of Ni (II) from electroplating wastewater. *Journal of hazardous materials*, *79*(1-2), 117-131.

[25] Lagergren, S. (1898). Zur theorie der sogenannten adsorption geloster stoffe. *Kungliga svenska vetenskapsakademiens. Handlingar*, *24*, 1-39.

[26] Khan, M. A., Ngabura, M., Choong, T. S., Masood, H., & Chuah, L. A. (2012). Biosorption and desorption of Nickel on oil cake: Batch and column studies. *Bioresource technology*, *103*(1), 35-42.

[27] Din, M. I., & Mirza, M. L. (2013). Biosorption potentials of a novel green biosorbent Saccharum bengalense containing cellulose as carbohydrate polymer for removal of Ni (II) ions from aqueous solutions. *International journal of biological macromolecules*, *54*, 99-108.

[28] Ho, Y. S. (2006). Second-order kinetic model for the sorption of cadmium onto tree fern: a comparison of linear and non-linear methods. *Water research*, *40*(1), 119-125.

[29] Mondal, B. C., Das, D., & Das, A. K. (2002). Synthesis and characterization of a new resin functionalized with 2-naphthol-3, 6-disulfonic acid and its application for the speciation of chromium in natural water. *Talanta*, *56*(1), 145-152.

[30] Kolcu, F. (2019). Characterization and spectroscopic study of enzymatic oligomerization of phenazopyridine hydrochloride. *Journal of Molecular Structure*, *1188*, 76-85.

[31] Wang, W., Lin, J., & Schwartz, D. C. (1998). Scanning force microscopy of DNA molecules elongated by convective fluid flow in an evaporating droplet. *Biophysical journal*, *75*(1), 513-520.

[32] Dutta, S., Bhaumik, A., & Wu, K. C. W. (2014). Hierarchically porous carbon derived from polymers and biomass: effect of interconnected pores on energy applications. *Energy & Environmental Science*, *7*(11), 3574-3592.

[33] Wang, L. C., Chen, X. G., Liu, C. S., Li, P. W., & Zhou, Y. M. (2008). Dissociation behaviors of carboxyl and amine groups on carboxymethyl-chitosan in aqueous system. *Journal of Polymer Science Part B: Polymer Physics*, *46*(14), 1419-1429.

[34] Doshi, B., Repo, E., Heiskanen, J. P., Sirviö, J. A., & Sillanpää, M. (2017). Effectiveness of N, O-carboxymethyl chitosan on destabilization of Marine Diesel, Diesel and Marine-2T oil for oil spill treatment. *Carbohydrate polymers*, *167*, 326-336.

[35] Orth, E. S., Ferreira, J. G., Fonsaca, J. E., Blaskievicz, S. F., Domingues, S. H., Dasgupta, A., & Zarbin, A.J. (2016). PKa determination of graphene-like materials: Validating chemical functionalization. *Journal of colloid and interface science*, *467*, 239-244.

[36] Basargin, N. N., Oskotskaya, E. R., Yushkova, E. Y., & Rozovskii, Y. G. (2006). Physicochemical properties of complexing para-substituted polystyrene sorbents containing functional amino groups. *Russian Journal of Physical Chemistry*, *80*(1), 115-119.

[37] Po, H. N., & Senozan, N. M. (2001). The Henderson-Hasselbalch equation: its history and limitations. *Journal of Chemical Education*, *78*(11).

[38] Leyva-Ramos, R. (1989). Effect of temperature and pH on the adsorption of an anionic detergent on activated carbon. *Journal of Chemical Technology & Biotechnology*, *45*(3), 231-240.

[39] Özcan, A. S., Erdem, B., & Özcan, A. (2004). Adsorption of Acid Blue 193 from aqueous solutions onto Na–bentonite and DTMA–bentonite. *Journal of Colloid and Interface Science*, *280*(1), 44-54.

[40] Altınışık, A., Gür, E., & Seki, Y. (2010). A natural sorbent, Luffa cylindrica for the removal of a model basic dye. *Journal of hazardous materials*, *179*(1-3), 658-664.

[41] Bulut, E., Özacar, M., & Şengil, İ. A. (2008). Adsorption of malachite green onto bentonite: equilibrium and kinetic studies and process design. *Microporous and mesoporous materials*, *115*(3), 234-246.

[42] Chen, C., & Wang, X. (2006). Adsorption of Ni (II) from aqueous solution using oxidized multiwall carbon nanotubes. *Industrial & Engineering Chemistry Research*, *45*(26), 9144-9149.

[43] Wang, L., Wu, X. L., Xu, W. H., Huang, X. J., Liu, J. H., & Xu, A. W. (2012). Stable organic–inorganic hybrid of polyaniline/α-zirconium phosphate for efficient removal of organic pollutants in water environment. *ACS applied materials & interfaces*, *4*(5), 2686-2692.

[44] Crini, G., & Peindy, H. N. (2006). Adsorption of CI Basic Blue 9 on cyclodextrin-based material containing carboxylic groups. *Dyes and Pigments*, *70*(3), 204-211.

[45] Tan, X., Wang, X., Fang, M., & Chen, C. (2007). Sorption and desorption of Th (IV) on nanoparticles of anatase studied by batch and spectroscopy methods. *Colloids and Surfaces A: Physicochemical and Engineering Aspects*, *296*(1-3), 109-116.

[46] Gupta, V. K., Jain, R., Shrivastava, M., & Nayak, A. (2010). Equilibrium and thermodynamic studies on the adsorption of the dye tartrazine onto waste “coconut husks” carbon and activated carbon. *Journal of Chemical & Engineering Data*, *55*(11), 5083-5090.

[47] Hosseini-Bandegharaei, A., Hosseini, M. S., Jalalabadi, Y., Sarwghadi, M., Nedaie, M., Taherian, A., ... & Eftekhari, A. (2011). Removal of Hg (II) from aqueous solutions using a novel impregnated resin containing 1-(2-thiazolylazo)-2-naphthol (TAN). *Chemical Engineering Journal*, *168*(3), 1163-1173.

[48] Genç-Fuhrman, H., Tjell, J. C., & McConchie, D. (2004). Adsorption of arsenic from water using activated neutralized red mud. *Environmental science & technology*, *38*(8), 2428-2434.

[49] Altundoğan, H. S., Altundoğan, S., Tümen, F., & Bildik, M. (2000). Arsenic removal from aqueous solutions by adsorption on red mud. *Waste Management*, *20*(8), 761-767.